

NJC

Accepted Manuscript



This is an *Accepted Manuscript*, which has been through the Royal Society of Chemistry peer review process and has been accepted for publication.

Accepted Manuscripts are published online shortly after acceptance, before technical editing, formatting and proof reading. Using this free service, authors can make their results available to the community, in citable form, before we publish the edited article. We will replace this *Accepted Manuscript* with the edited and formatted *Advance Article* as soon as it is available.

You can find more information about *Accepted Manuscripts* in the [Information for Authors](#).

Please note that technical editing may introduce minor changes to the text and/or graphics, which may alter content. The journal's standard [Terms & Conditions](#) and the [Ethical guidelines](#) still apply. In no event shall the Royal Society of Chemistry be held responsible for any errors or omissions in this *Accepted Manuscript* or any consequences arising from the use of any information it contains.

A highly selective and biocompatible chemosensor for sensitive detection of zinc(II)

Sudipto Dey^a, Ankita Roy^a, Guru Prasad Maiti^b, Sushil Kumar Mandal^c, Piyali Banerjee^a and Partha Roy^{*,a}

^a Department of Chemistry, Jadavpur University, Jadavpur, Kolkata-700 032, India.

E-mail: proy@chemistry.jdvu.ac.in; Tel: +91-33-2457-2970; Fax: +91-33-2414-6414.

^b Department of Molecular Biology and Biotechnology, University of Kalyani, Kalyani-741235, West Bengal, India.

^c Department of Ecological Engineering & Environmental Management, University of Kalyani, Kalyani, Nadia-741235, West Bengal, India.

Abstract:

2-Formyl-4-methyl-6-(2-benzoimidazolyliminomethyl)phenol (HL¹) has been synthesized by Schiff-base condensation between 4-methyl-2,6-diformylphenol and 2-aminobenzimidazole in 1:1 ratio in acetonitrile and characterized by elemental analysis and different spectroscopic methods. HL¹ has been found to be selective fluorescence sensor for Zn²⁺ ion. Emission intensity of HL¹ at 528 nm in 10 mM HEPES buffer in water:methanol (1:9, v/v) (pH = 7.2) increases in the presence of Zn²⁺ when it is excited at 445 nm. Other metal ions can induce slight increment or lowering of emission intensity. Spectral properties of HL¹ and 2-formyl-4-methyl-6-(2-benzoimidazolymethyliminomethyl)phenol (HL²) have been compared. It has been found that the presence of methylene group in HL² can significantly effect on absorption and fluorescence peak positions of the Schiff-base molecule and its zinc complex. Some theoretical calculations have been done to get a better view into the different spectral transitions. HL¹ and HL² have been found to be highly sensitive towards the detection of Zn²⁺ ion with very low LOD values. Excitation in visible region and effect of pH on emission intensity of HL¹ encourage us for the biological study. HL¹ has been used for human lung cancer cell (A549) imaging without cytotoxicity.

Introduction

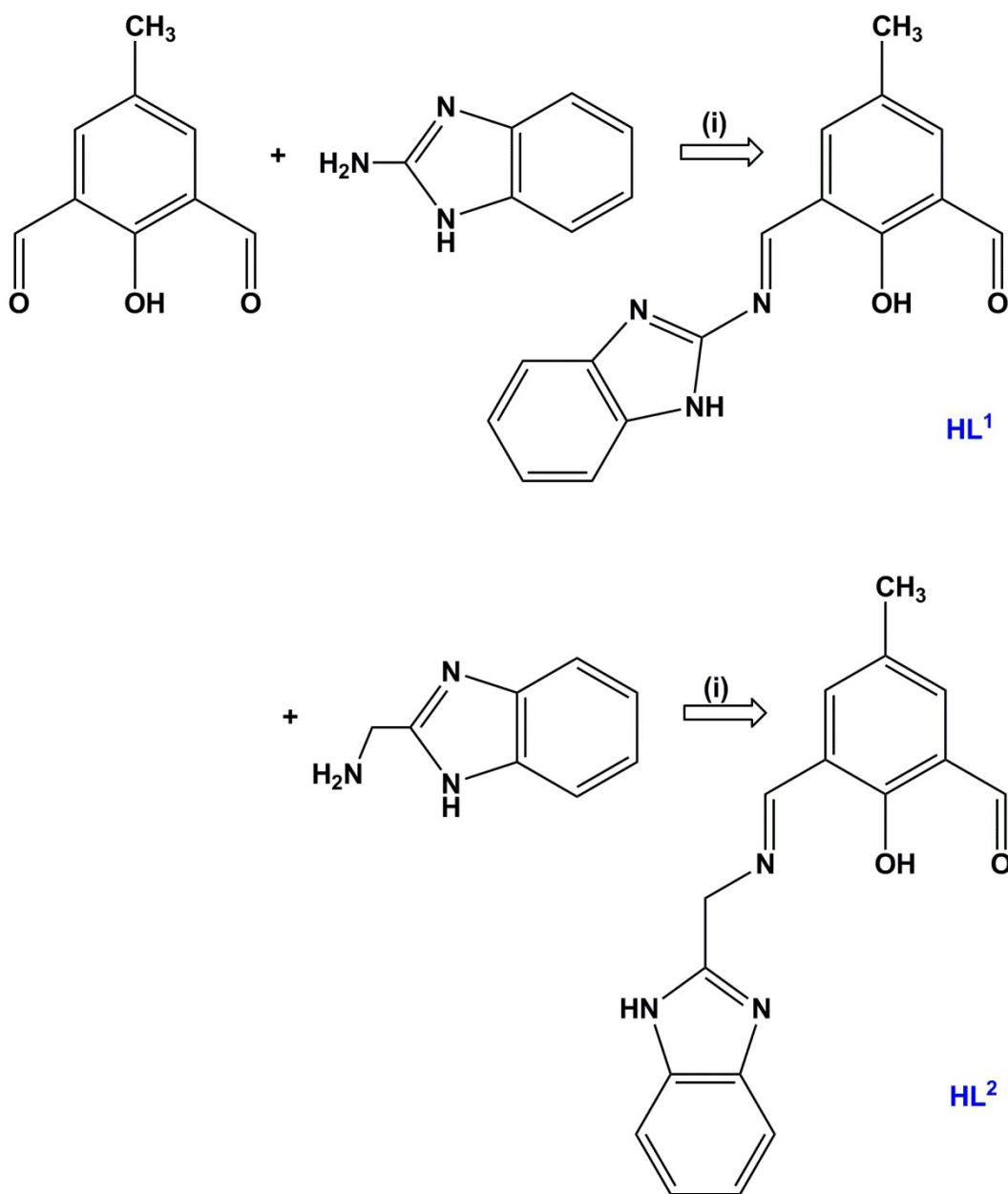
Zinc is one of the most abundant metal ions in our body system. Research on Zn^{2+} ion has become hotspot in chemical sciences as well as in biological sciences because of biological relevance of the metal ion. It is essential component of many enzymes. It plays a significant role in maintaining key structure of gene transcription protein e.g. zinc finger protein.^{1,2} Besides, it regulates neuronal transmission in excitatory nerve terminal,³ and suppresses apoptosis,⁴ epilepsy⁵ and transient global ischemia.⁶ Moreover, it induces amyloid formation which is reported to be one of the key factors related to the Alzheimer's disease.⁷ Zn^{2+} ion is nontoxic in nature. However, considerable amount of it within human body may lead to severe toxicity. So detection and determination of Zn^{2+} is very important from medical point of view. Vesicles in synapse in excitatory nerve terminals are rich with high concentration of chelatable Zn^{2+} , which is discharged due to neuronal activity.⁸ Although it is recognized that the metal ion has many key cellular functions but its physiological importance is not still completely understood. On the other hand, zinc is a pollutant metal which decreases activity of the soil microbes.^{9,10} This metal ion is a common contaminant in agriculture and food waste. Its inclusion in food chain and consequent human consumption can give rise to a number of diseases, e.g. pulmonary manifestation, fever and gastroenteritis.¹¹

Thus, highly efficient and selective tools for detection and measurement of Zn^{2+} ion become essential. Several analytical techniques such as UV–Vis spectroscopy, potentiometry and flame atomic absorption spectrometry, inductivity coupled plasma atomic emission spectroscopy (ICPAES) and fluorescence method have been applied for zinc ion assay in various samples. The available detection methods of Zn^{2+} are still limited. However, due to its d^{10} electronic configuration of Zn^{2+} , fluorescence spectroscopy becomes only method to detect and measure Zn^{2+} ion.

Up to now, most available probes detect Zn^{2+} *via* measuring the metal-induced changes in fluorescence intensity based on photo-induced electron transfer (PET). Quinolines and their derivatives have been used traditionally as fluorogenic agents for the chemical assay of Zn^{2+} .¹² It is regarded as a milestone in the development of fluorescent probes for biological Zn^{2+} when 6-methoxy-8-p-toluenesulfonamido-quinoline (TSQ)¹³ was first applied for imaging Zn^{2+} *in vitro* in 1987. A significant amount of research work on the development of fluorescein based fluorescence sensor for Zn^{2+} has been reported so far.¹⁴⁻¹⁷ Different fluorescence sensors based

on coumarin, rhodamine, etc. for Zn^{2+} are being reported till now.¹⁸⁻²⁵ These sensor molecules have successfully applied for cell imaging studies. A fluorescence sensor based on another fluorophore, namely, 4-methyl-2,6-diformylphenol (DFP) for Zn^{2+} was reported quite few years back.²⁶ After that some other groups have also reported sensors based on (DFP).^{27,28} Recently, half-condensed Schiff-base molecule of DFP has been used for detection of Zn^{2+} and Mg^{2+} .²⁹ The sensing mechanism is due to the combined effect of inhibition of excited state intramolecular proton transfer (ESIPT), CH=N isomerization and chelation enhanced fluorescence (CHEF). A recently published research article shows that a Schiff-base compound derived from salicylaldehyde acts as ratiometric sensor for Zn^{2+} and Al^{3+} . A Schiff-base molecule of pyridoxal has been used for the detection of Zn^{2+} ion. The mechanism of the probe for Zn^{2+} is due to combined effects of C=N isomerization and CHEF.³⁰ A multi-metal colorimetric and fluorescent sensor based on Schiff base of salicylaldehyde derivative has been developed where probe can detect Zn^{2+} by fluorescence spectrometry and few others metal ion along with Zn^{2+} by colorometric method.³¹ An amino acid Schiff base based on isomerization of C=N is capable of recognizing Zn^{2+} ions selectively and sensitively in aqueous medium.³² But all of these reports of different Schiff-bases based Zn^{2+} sensors possess some limitations e.g. low excitation wavelength, unknown limit of detection etc. There is scope of improvement of selectivity and sensitivity for Zn^{2+} ion by Schiff-base molecules with DFP.

In this context, we report here a new Schiff-base compound, 2-formyl-4-methyl-6-(2-benzoimidazolyliminomethyl)phenol (HL^1), derived from 4-methyl-2,6-diformylphenol as a fluorescence Zn^{2+} sensor (Scheme 1). HL^1 was prepared by Schiff-base condensation between 4-methyl-2,6-diformylphenol and 2-aminobenzimidazole in 1:1 ratio in acetonitrile. It was characterized by elemental analysis and different spectroscopic methods. It shows about 8 times increment in emission intensity in the presence of one equivalence of Zn^{2+} ion when it is excited at 445 nm. Cd^{2+} and Hg^{2+} induce slight increase in emission intensity whereas all other relevant metal ions either decreased or unchanged intensity. To examine effect of methylene group on the fluorescence sensing properties of HL^1 , we have introduced one methylene group to get another Schiff-base, 2-formyl-4-methyl-6-(2-benzoimidazolylmethyliminomethyl)phenol (HL^2). Comparison of spectral properties and some theoretical calculations on both the compounds are also reported here. LOD of the Schiff-base molecules has been determined. HL^1 has been used to image human lung cancer cell without any cytotoxicity.



Scheme 1: Synthetic route to HL¹ and HL²: (i) = acetonitrile, reflux 4 h.

Experimental Sections

Materials and methods

2-aminobenzimidazole, 2-aminomethylbenzimidazole and HEPES, sodium salt were purchased from Sigma Aldrich and used as received. Other reagents were purchased from

commercial source and used without further purification. 4-methyl-2,6-diformylphenol was synthesized following a published procedure.³³ Solvents used for spectroscopic studies were purified and dried by standard procedures before use.³⁴ Elemental analysis was carried out in a 2400 Series-II CHN analyzer, Perkin Elmer, USA. FT-IR spectra were recorded on a Perkin Elmer spectrometer (Spectrum Two) with the samples by attenuated total reflectance (ATR) technique. Absorption spectra were studied on a Shimadzu UV 2100 spectrophotometer. Emission spectra were recorded on PTI made fluorescence spectrometer (Model no. QM-40). The ESI-MS⁺ spectra were recorded on a QTOF Micro YA263 mass spectrometer. NMR spectra of the compounds were recorded on either Bruker 500 MHz spectrometer or Bruker 300 MHz spectrometer using DMSO-d₆ as solvent. Luminescence lifetime measurements were performed using a TCSPSC (time-correlated single photon counting) set up from Horiba Jobin-Yvon. The luminescence decay data were recorded on a Hamamatsu MCP photomultiplier (R3809) and were analyzed using the IBH DAS6 software.

Emission quantum yields (Φ) of HL and its Zn²⁺ complex were measured by using the formula:

$$\Phi_{\text{sample}} = \left\{ \frac{(\text{OD}_{\text{standard}} \times A_{\text{sample}} \times \eta_{\text{sample}}^2)}{(\text{OD}_{\text{sample}} \times A_{\text{standard}} \times \eta_{\text{standard}}^2)} \right\} \times \Phi_{\text{standard}}$$

where A is the area under the emission spectral curve, OD is optical density of the compound at the excitation wavelength and η is the refractive index of the solvent, quantum yield of standard (here fluorescein.) is 0.91 ($\lambda_{\text{ex}} = 470 \text{ nm}$).³⁵

A549, human lung cancer cell lines were obtained from National Center for Cell Science, Pune, India, and used throughout the experiments. Cells were cultured in DMEM (Himedia) supplemented with 10% FBS (Himedia), and an antibiotic mixture (1%) containing PSN (Himedia) at 37°C in a humidified incubator with 5% CO₂ and cells were grown to 80-90% confluence, harvested with 0.025% trypsin (Himedia) and in phosphate-buffered saline (PBS), plated at the desired cell concentration and allowed to grow overnight before any treatment.

Synthesis of 2-formyl-4-methyl-6-(2-benzoimidazolyliminomethyl)phenol (HL¹) and 2-formyl-4-methyl-6-(2-benzoimidazolylmethyliminomethyl)phenol (HL²)

HL¹ and HL² were synthesized following a similar procedure. In general, 0.082 g (0.50 mmol) of 4-methyl-2,6-diformylphenol in 5 mL of acetonitrile was added to 0.50 mmol respective amine (0.066 g of 2-aminobenzimidazole for HL¹ and 0.073 g of 2-

aminomethylbenzimidazole for HL²) in 5 mL of acetonitrile taken in a round bottom flask. The solution was stirred for 15 min and then allowed to reflux for 4 h. The reaction mixture was cooled to room temperature. The solution was allowed to stand overnight at room temperature when solid product was precipitated. The product was collected by filtration, washed with small amount of acetonitrile and dried in vacuum.

Data for HL¹: Yield (85%); C, H, N analysis: *Anal. Calc.* for C₁₆H₁₃N₃O₂: C, 68.81; H, 4.70; N, 15.04; Found: C, 68.74; H, 4.57; N, 14.98%. ESI-MS⁺ (*m/z*): 280.12 (HL¹ + H⁺); FT-IR (Wave number, cm⁻¹) 3166, 1658, 1585, 1431, 1235, 972, 733 (Figure 2); ¹H-NMR (in DMSO-d⁶) (d, ppm): 2.34 (s, 3H), 7.19–7.23 (m, 2H), 7.50–7.60 (m, 2H), 7.74 (s, 1H), 7.99 (s, 1H), 9.65 (s, 1H); 10.41 (s, 1H); 12.87 (s, 1H).

Data for HL²: Yield (94%); C, H, N analysis: *Anal. Calc.* for C₁₆H₁₃N₃O₂: C, 69.61; H, 5.15; N, 14.33; Found: C, 69.51; H, 5.06; N, 14.38%. ESI-MS⁺ (*m/z*): 294.11 (HL² + H⁺); ¹H-NMR (in DMSO-d⁶) (d, ppm): 2.34 (s, 3H), 4.52 (s, 2H), 7.22–7.28 (m, 2H), 7.62–7.72 (m, 2H), 7.88 (s, 1H), 8.14 (s, 1H), 9.82 (s, 1H), 10.54 (s, 1H), 13.02 (s, 1H).

Computational details

DFT calculations on HL¹, HL² and their Zn²⁺ complexes (complexes 1 and 2) were fully optimized using Gaussian 03 program.³⁶ The B3LYP functional has been adopted along with the 6-31G basis set for H, C, N, O atoms and LANL2DZ effective core potentials and basis set for the Zn atom. The global minima of all these species were authenticated by the positive vibrational frequencies. Time dependent density functional theory (TDDFT) with B3LYP density functional was applied to study the low-lying excited states of the complex in methanol.³⁷⁻⁴⁰ The UV spectra were computed from TDDFT calculations in methanol.

Cell imaging study

A549 cells were cultured and cells were rinsed with PBS and incubated with DMEM containing HL¹ making the final concentration up to 10 μM in DMEM [the stock solution (3 mM) was prepared by dissolving HL¹ into DMSO] for 30 min at 37°C. After incubation, bright field and fluorescence images of A549 cells were captured by a fluorescence microscope (Model: LEICA DM4000B, Germany) with an objective lens of 20X magnification. Similarly, fluorescence images of A549 cells (pre-incubated with 10 μM of HL¹) were taken with addition

of different concentrations (10 μ M-50 μ M) of zinc nitrate salt at 10 minute interval. A merged image between phase contrast and fluorescent images at 50 μ M salt concentration were taken and consequently fluorescence images were taken after further addition of TPEN (100 μ M).

Cell cytotoxicity assay:

In order to test the cytotoxicity of HL¹ in absence and in the presence of Zn²⁺, 3-(4, 5-dimethylthiazol-2-yl)-2,S-diphenyltetrazolium bromide (MTT) assay was done in A549 cells according to standard procedure.⁴¹ Briefly, after treatment of A549 cells (10³ cells in each well of 96-well plate) with HL¹ (1, 10, 20, 50 and 100 μ M) for 6 h, 10 μ l of a MTT solution (1 mg/ml in PBS) was added in each well and incubated at 37°C continuously for 3 h. All media were removed from wells and 100 μ l of acidic isopropyl alcohol was added into each well. The intracellular formazan crystals (blue-violet) formed were solubilized with 0.04 N acidic isopropyl alcohol and absorbance of the solution was measured at 595 nm wavelength with a microplate reader (Model: THERMO MULTI SCAN EX). The cell viability was expressed as the optical density ratio of the treatment to control. Values are mean \pm standard deviation of three independent experiments. The cell cytotoxicity was calculated as % cell cytotoxicity = 100% - % cell viability.

Results and discussion

Synthesis and characterization

HL¹ and HL² were synthesized by following similar procedure (Scheme 1). The compounds were synthesized by the condensation of 1 equiv. of 4-methyl-2,6-diformylphenol with 1 equiv. of respective amine (2-aminobenzimidazole for HL¹ and 2-aminomethylbenzimidazole for HL²) in acetonitrile. One of two CHO groups of 4-methyl-2,6-diformylphenol reacts with the amine. The product was collected as solid in good yield. It was characterized by elemental analysis and different spectroscopic methods. Mass spectra of both the compounds were recorded methanol (Fig. s1 and s2). Mass spectrum of HL¹ shows an *m/z* peak at 280.12 which can be attributed to the presence of the compound. Similarly, mass spectrum of HL² exhibits peak at 294.11. HL¹ and HL² form complexes with Zn²⁺ in 1:1 ratio (Fig. s3 and s4) and designated as complex 1 {[Zn(L¹)(CH₃OH)(H₂O)]⁺} and complex 2 {[Zn(L²)(CH₃OH)(H₂O)]⁺}, respectively. Characterization of Schiff-base molecules has been

done with ^1H NMR spectroscopy. Details for HL^1 have discussed later whereas ^1H NMR spectrum of HL^2 shows the signals for the presence of $-\text{CHO}$ and methylene protons (Fig. s5). Presence of one formyl group is evident from FT-IR spectra of HL^1 and HL^2 (Fig. s6 and s7). FT-IR spectrum of HL^1 shows a broad band at around 3169 cm^{-1} due to the presence of phenolic OH group. The sharp bands at 1663 cm^{-1} may be attributed to the presence of CHO group whereas bands at 1624 and 1582 cm^{-1} may be attributed to C=N moieties. FT-IR spectrum of HL^2 shows similar bands. IR spectrum of it exhibits bands at 3190 (br, for phenolic OH), 1662 (for CHO), 1636 and 1597 cm^{-1} (for azomethine).

Main focus will be on the spectral properties and selective Zn^{2+} sensing behavior of HL^1 . Discussion on HL^2 has been made when properties of HL^1 and HL^2 are being compared.

Absorption spectral studies

The mode of interaction of HL^1 with Zn^{2+} was investigated by spectrophotometric titration in 10 mM HEPES buffer in water:methanol (1:9, v/v) (pH = 7.2) at 25°C (Fig. 1). It shows a peak at 387 nm. Upon gradual addition of Zn^{2+} ion, the intensity at 387 nm decreases and at the same time a new peak at around 445 nm emerges. It can be seen from the figure that upon addition of about one equivalence of Zn^{2+} , the intensity at 387 nm decreases significantly with a prominent peak at 445 nm. During addition of Zn^{2+} isosbestic points develop at 320 and 416 nm. The new absorption band indicates the binding of HL^1 with Zn^{2+} ion. The donor atoms in the Schiff-base binds to Zn^{2+} to form a chelate ring, as a result the conjugation in the system is extended resulting the new absorption in the longer wavelength.⁴² The intensity of peak at 250 nm also decreases with the increase in metal concentration. Another two isosbestic points have been generated at 242 and 260 nm. All of these phenomena show transformation of free Schiff-base ligand into Zn(II)–Schiff-base complex.

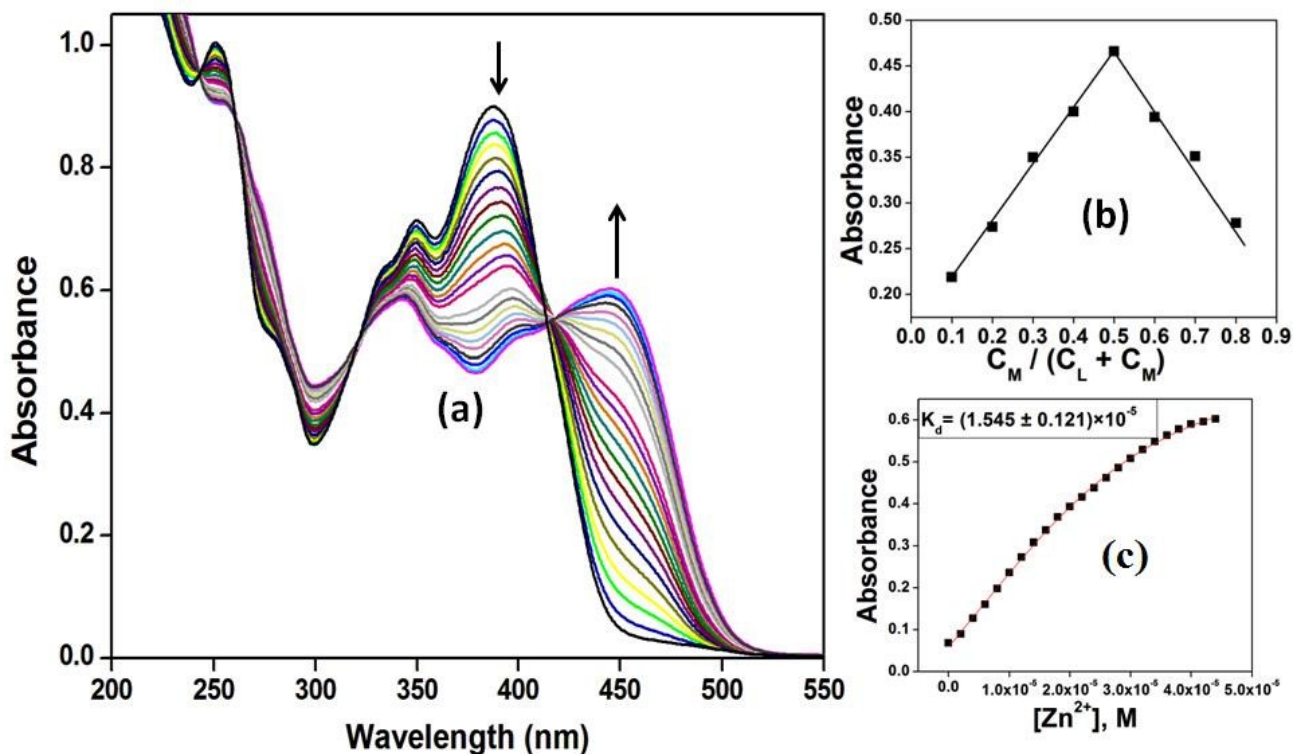


Fig. 1: (a) Absorption spectra of HL¹ (40 µM) with the gradual addition of Zn²⁺ ion (0-40 µM) in 10 mM HEPES buffer in water:methanol (1:9, v/v) (pH = 7.2) at room temperature; (b) Job's plot indicating 1:1 complex formation and (c) Plot of absorption at 445 nm vs. concentration of Zn²⁺.

Similar observation of UV-vis spectrum of HL² in the presence of Zn²⁺ has been noticed (Fig. s8). Interaction of HL² with Zn²⁺ has been investigated in 10 mM HEPES buffer in water:methanol (1:9, v/v) (pH = 7.2) at 25°C (Fig. s8). UV-vis spectrum of HL² shows band at 342 nm. On gradual addition Zn²⁺ ion to it, intensity at 342 decreases while a new peak at 398 nm appears. An isosbestic point at 360 nm has been noticed.

It is interesting to note that the presence of methylene group has a visible effect on UV-visible spectrum of the Schiff-base compound. Absorption band of HL¹ at 387 nm has shifted to 342 nm in HL² due to the mere presence of one methylene group. Actually, the presence of methylene group in HL² destroys the conjugation present in benzimidazole and phenyl rings of HL¹. The effect is also evident in absorption spectrum of HL¹ in the presence of Zn²⁺. In the presence of Zn²⁺, HL¹ and HL² show bands at 445 and 398 nm respectively.

Job's plot analysis indicates 1:1 binding of Zn^{2+} with both the ligands separately. 1:1 binding of Zn^{2+} with both the ligands is well supported by the mass spectra analysis (Fig. 1 and Fig. s8).

The geometries of the Schiff-base ligands HL^1 and HL^2 , and complexes 1 and 2 were fully optimized by DFT/B3LYP method using the Gaussian 03 program. The experimental data and our calculated structural parameters are quite similar. Geometry optimized structures of all the compounds are given in Fig. 2. Some selected optimized geometrical parameters of complexes 1 and 2 are listed in Table s1. The modeled geometry of complex 1 and complex 2 possess a distorted tetrahedral arrangement around the central metal ion Zn with N,O donor atoms of the ligands. In complex 1, all the calculated Zn–O/Zn–N distances fall in the range of 2.001–2.086 Å but for complex 2 calculated Zn–O/Zn–N distances fall in the range of 2.074–2.091 Å (Table s1). The contour plots of preferred Frontier molecular orbitals of complexes 1 and 2 are given in Fig. s9.

For better understanding of the electronic transitions of our complexes, time dependent density functional theory i.e TDDFT calculations have been carried out at the B3LYP associated with the conductor-like polarizable continuum model (CPCM) method in methanol using the optimized geometry of the ground (S_0) state. The complex 1 shows moderately broad peak at 442 nm (445 nm experimental) dominated by HOMO→LUMO transition, moderately intense peak at 382 nm (387 nm experimental) due to HOMO-1→LUMO and HOMO→LUMO+1 transitions and at 347 nm (350 nm experimental) due to HOMO-2→LUMO, HOMO-1→LUMO+2 transitions and at 247nm (251 nm experimental) .The complex 2 shows broad peak at 398 nm (experimental 400 nm) dominated by HOMO→LUMO transition, intense peak at 346 nm (experimental 342 nm) due to HOMO-2→LUMO, HOMO-2→LUMO+1 transitions and a moderately intense peak at 274 nm (272 nm experimentally) due to HOMO-5→LUMO, HOMO-2→LUMO+1 transitions (Fig. 3; Table s2). The HOMO-LUMO energy gap clearly shows reason of higher λ_{max} for complex 1 than complex 2 (Fig. 4).

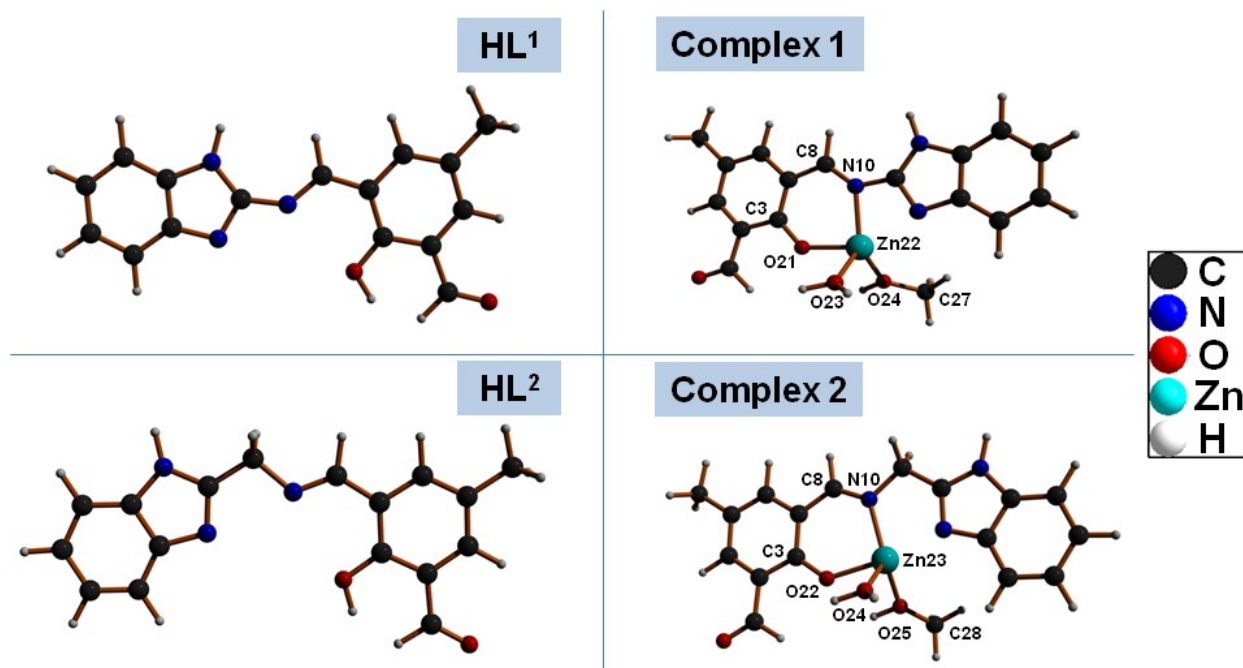


Fig. 2: Optimized geometries of HL¹, HL², complex 1 and complex 2 at their ground state (S_0).

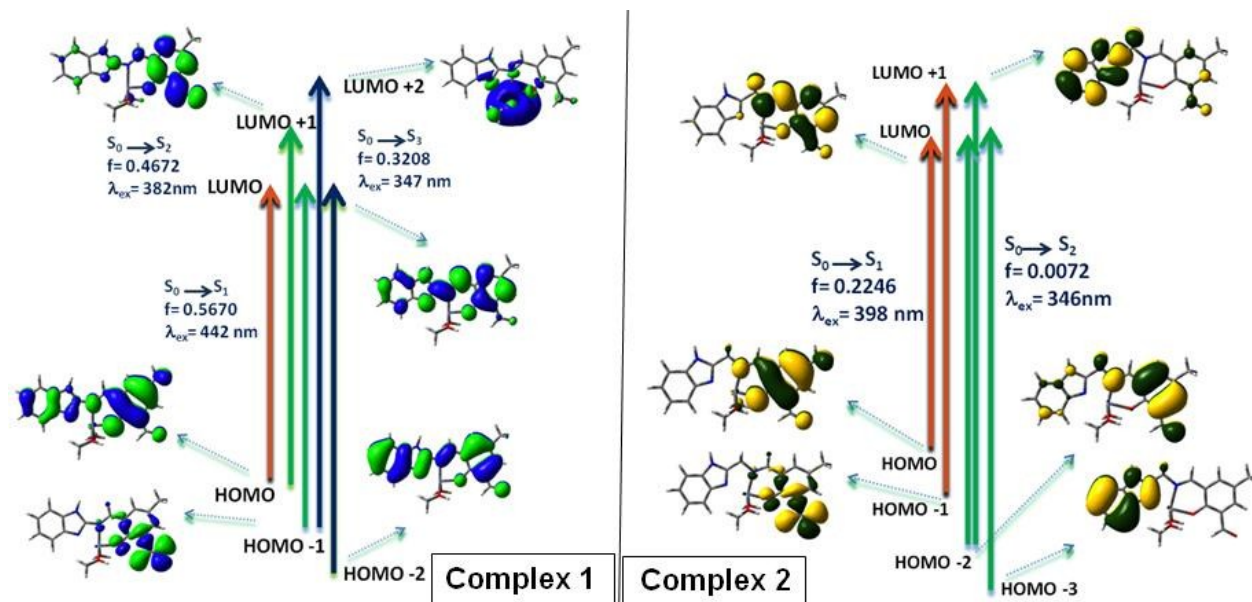


Fig. 3: Frontier molecular orbitals involved in the UV-vis absorption of complexes 1 and 2.

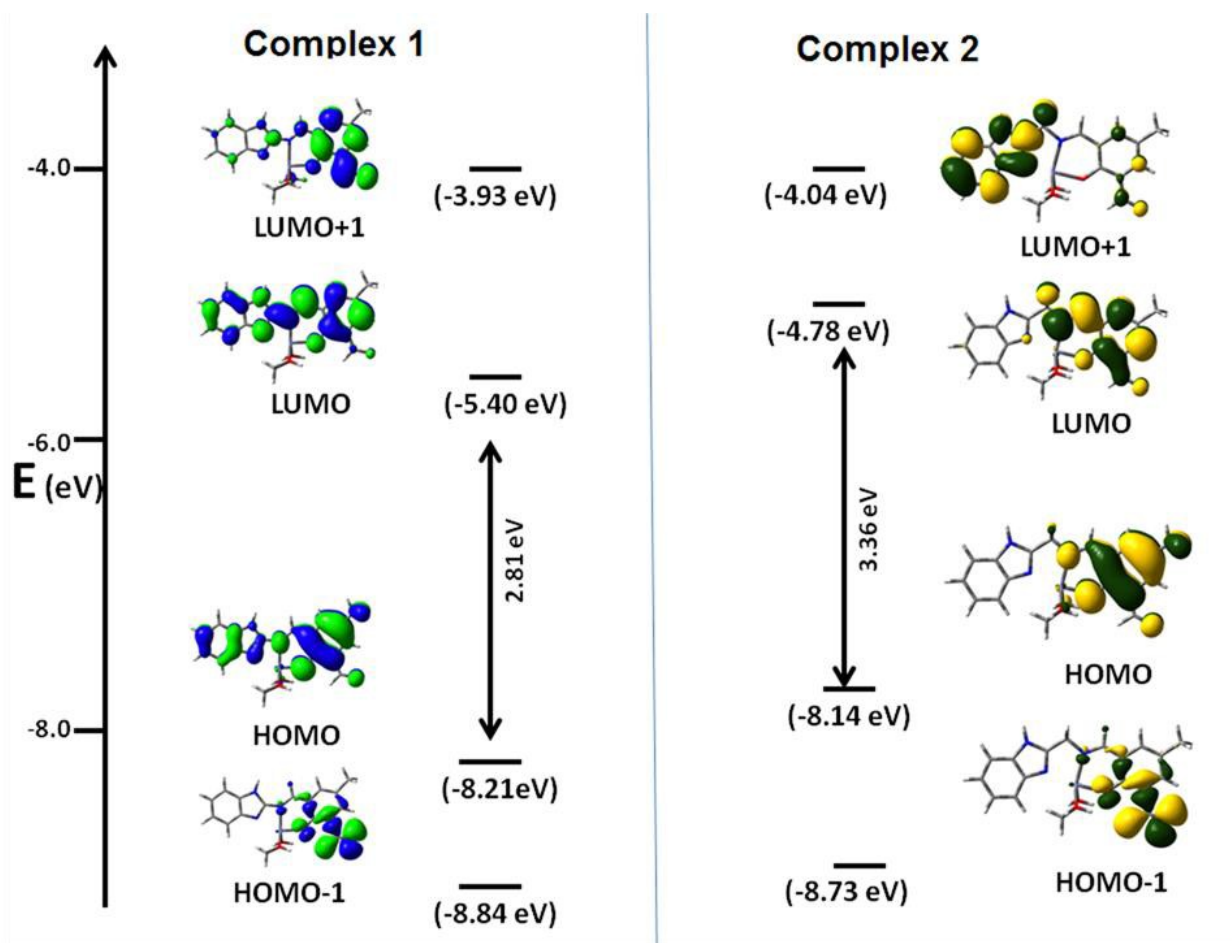


Fig. 4: Frontier MOs along with their HOMO- LUMO energy gap of complexes 1 and 2.

Fluorescence properties

HL¹ (40 μ M) shows weak fluorescent intensity at 528 nm when it has been excited at 445 nm in 10 mM HEPES buffer in water:methanol (1:9, v/v) (pH = 7.2) at room temperature. Emission intensity of HL¹ increases in the presence of Zn²⁺ ion (Fig. 5). Intensity of the Schiff-base compound at 528 nm gradually increases with the increase in concentration of Zn²⁺. Increment in intensity of HL¹ gets saturated when one equiv. of Zn²⁺ ion is added to it. There is about 8 fold enhancement in emission intensity of HL¹ in the presence of one equiv. of Zn²⁺. Similar observation has been noticed for HL² (Fig. s10). It shows weak fluorescent intensity at 478 nm on excitation at 398 nm in 10 mM HEPES buffer in water:methanol (1:9, v/v) (pH = 7.2) at room temperature. Emission intensity of HL² increases in the presence Zn²⁺ and saturates

when one eqv. of the metal ion is added. Emission intensity increase can be explained based on (Photoinduced Electron Transfer) PET mechanism (Fig. 6). Available lone pair on imine nitrogen atom keeps PET on leading to the quenching of fluorescence. When Zn^{2+} binds with Schiff-base compound, lone pair on nitrogen atom is no longer available thereby turning off PET and fluorescence is turned on. However, CHEF mechanism for increase of emission intensity cannot be totally ruled out as the binding constant of HL^1 towards Zn^{2+} is quite high.

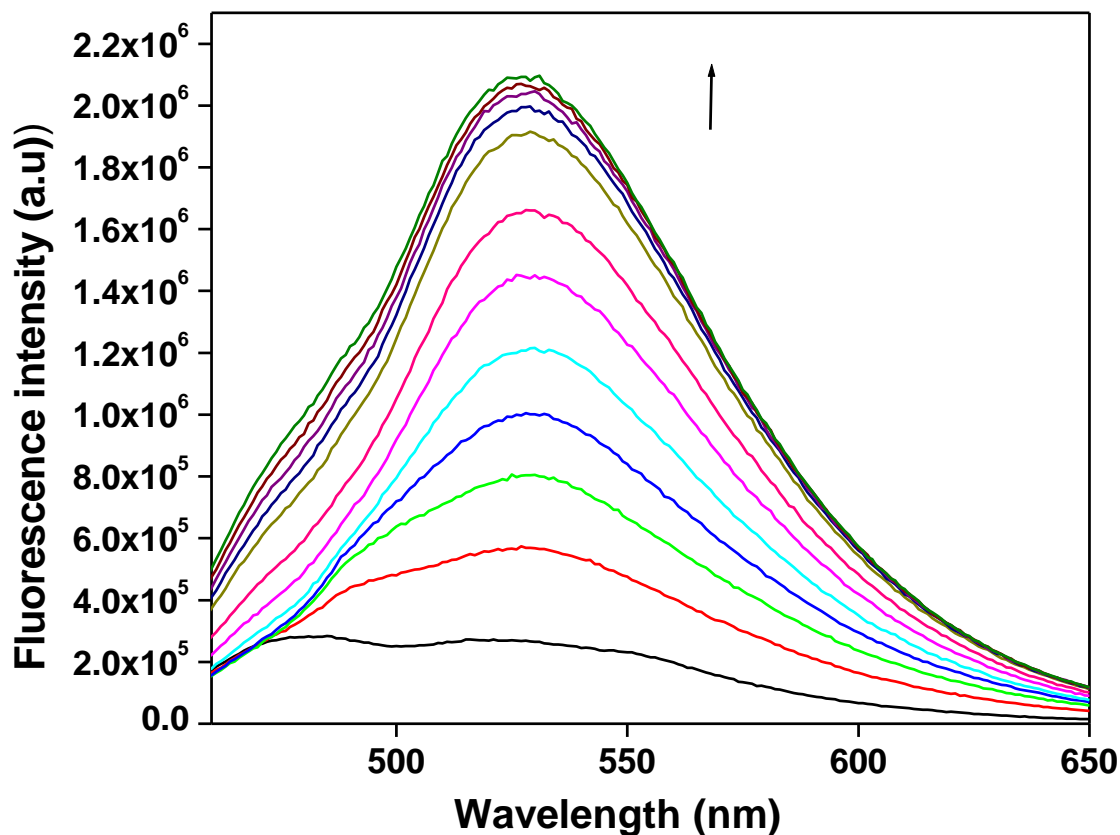


Fig. 5: Fluorescence intensity of HL^1 (40 μM) in the presence of 0, 4, 8, 12, 16, 20, 24, 28, 32, 36, 40 and 44 μM of Zn^{2+} ion in 10 mM HEPES buffer in water:methanol (1:9, v/v) (pH = 7.2) at room temperature (excitation: 445 nm).

HL^1 is not soluble in water alone. However, we have recorded UV-vis and fluorescence spectra in different water/methanol ratio (Fig. s11). With the increase in water percentage, emission intensity of HL^1 in the presence of Zn^{2+} decreases slowly. We have chosen water:methanol in 9:1 ratio.

Metal ion selectivity assay of HL¹ is shown in Fig. 7. Emission of HL¹ has been checked in the presence of various metal ions (5 equiv.). It is clear from the figure that only Zn²⁺ ion can induce significant fluorescence intensity enhancement. However, emission intensity of the

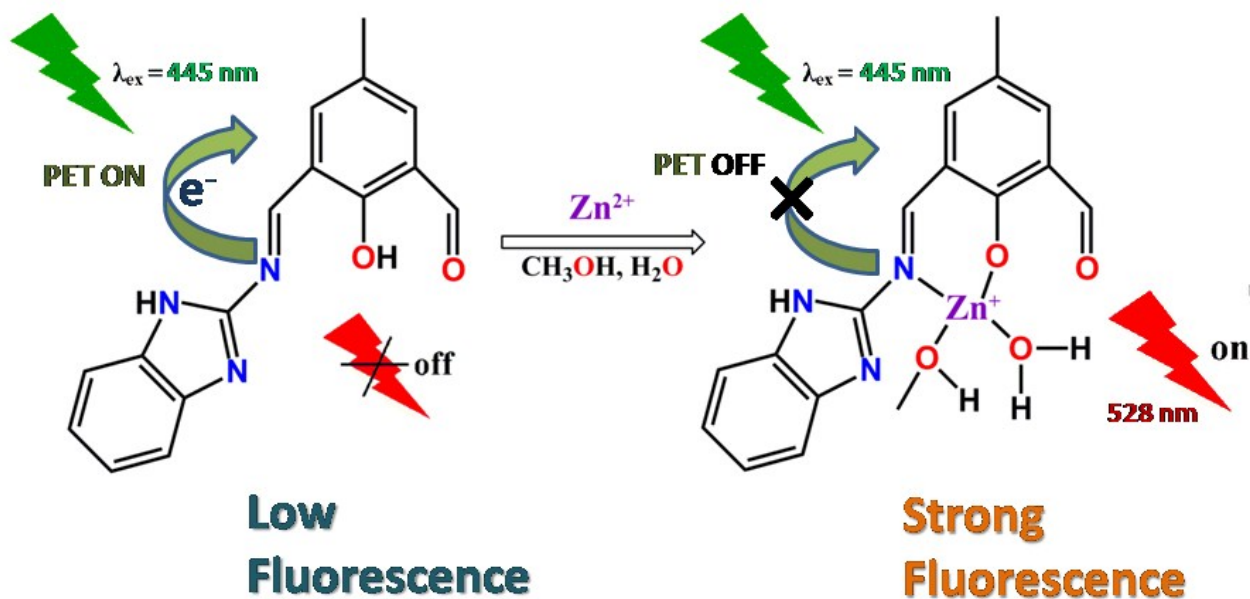


Fig. 6: Mechanism for increment of fluorescence intensity of HL¹ in the presence of Zn²⁺.

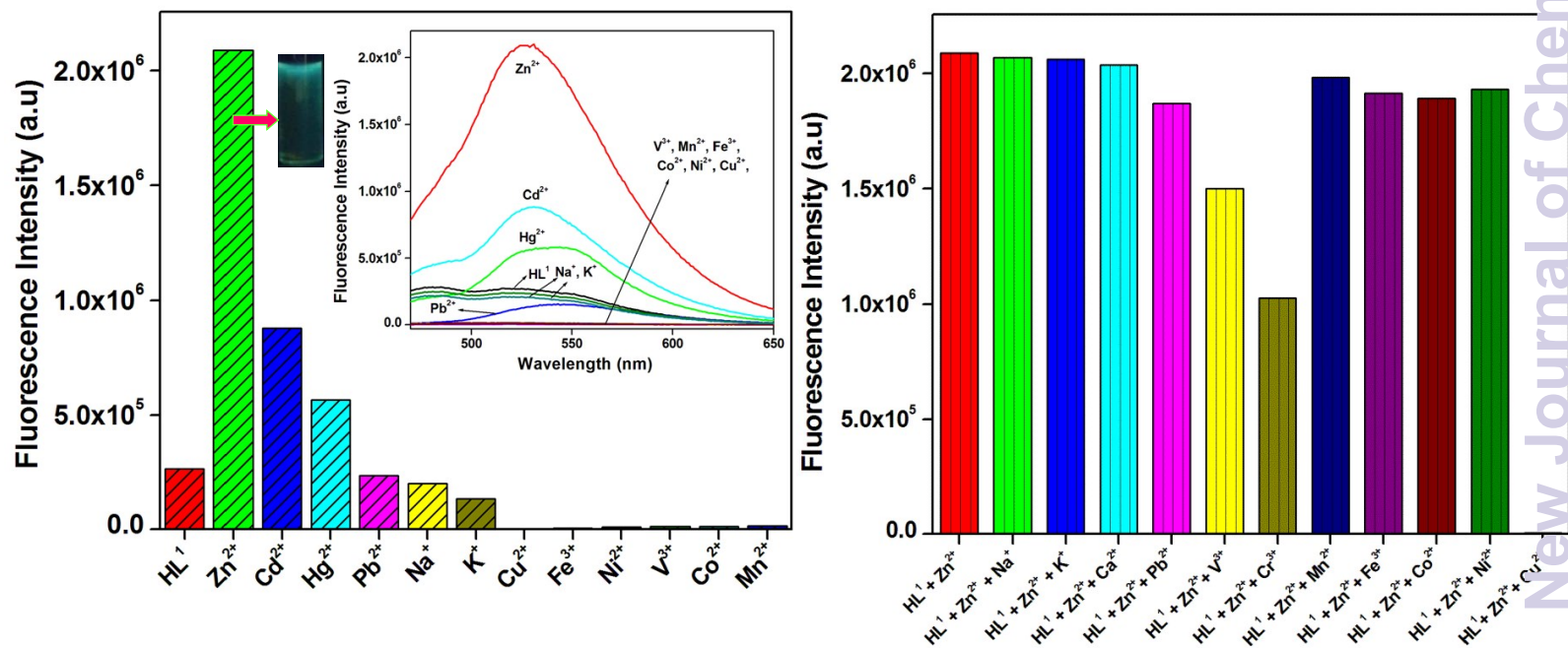


Fig. 7: Fluorescence intensity of HL¹ (40 μM) in the presence of different metal ions (200 μM) (left) and in the presence of mixture of metal ions including Zn²⁺ (right) in 10 mM HEPES buffer in water:methanol (1:9, v/v) (pH = 7.2) at room temperature (excitation: 445 nm).

compound increases slightly in the presence of two heavy metal ions of the same group of periodic table, Cd²⁺ and Hg²⁺. Alkali metal ions in large excess cannot induce emission increment. This may happen due to poor complex formation of HL¹ with the metal ions. The other first row transition metal ions, namely Cu²⁺, Fe³⁺, Ni²⁺, V³⁺, Co²⁺, and Mn²⁺ actually decrease emission intensity by the fluorescence quenching mechanism. Emission intensity of HL¹ and Zn²⁺ has been recorded in the presence of 5 eqv. of other metal ions (Fig. 7). It can be observed that emission intensity does not significantly changed in most of the cases. However, V³⁺ and Cr³⁺ can reduce intensity to some extent. 5 eqv. of Cu²⁺ reduce the emission intensity completely. Probably Cu²⁺ ion forms more stable complex than Zn²⁺. It replaces Zn²⁺ ion. Similar observation of effect of other metal ions in the fluorescence intensity of HL² has been recorded (Fig. s12).

To check influence of any anion on emission intensity, we have measured fluorescence intensity of HL¹ (40 μM) and Zn²⁺ ion in the presence of different counter anion (Fig. s13). It is revealed that there is no effect of various anions on emission intensity i.e. enhancement of intensity of HL¹ is due to the presence of metal ion only.

Enhancement of emission intensity of HL¹ in the presence of Zn²⁺ ion has been attributed to the large binding constant value. The binding constant has been determined by using Benesi-Hildebrand equation.^{43,44}

$$1/(F-F_0) = 1/(F_{\max}-F_0) + (1/K[C])\{1/(F_{\max}-F_0)\}$$

where F₀, F and F_{max} are emission intensities of HL¹ in absence of Zn²⁺, intermediate Zn²⁺ concentration and concentration of Zn²⁺ of complete interaction respectively; [C] is concentration Zn²⁺ and K is the binding constant. From a plot of (F_{max}-F₀)/(F-F₀) vs 1/[Zn²⁺] (Fig. s14), K for HL¹ was determined from the slope to be 4.38 (± 0.09) × 10⁴ M⁻¹.

Quantum yields of HL¹ and its Zn(II) complex have been determined (Table 1). From TCSPC (Time-Correlated Single Photon Counting) measurements, life-time of Schiff-base compounds and its Zn(II) complex have been determined (Fig. s15). From the figure it is evident that HL¹ undergoes bi-exponential decay whereas its zinc complex undergoes mono-exponential decay. Possibly due to the presence of different conformations of HL¹, bi-exponential decay is

observed. It may appear that its zinc complex also undergoes bi-exponential decay. But after close inspection, it can be understood that it is mono-exponential decay. However, initial decay of zinc complex matches with prompt profile which is due the unwanted scattering. The life times for them are measured to be 1.25 and 7.29 ns respectively.

Radiative and non-radiative decay constants were determined by following equations:

$$k_r = \Phi_f/\tau \text{ and } \tau^{-1} = k_r + k_{nr}$$

Table 1: Quantum yield, Life-time and rate constants of HL¹

| Compound | Quantum yield | Life-time (ns) | K _r (×10 ⁶) | K _{nr} (×10 ⁶) | χ ² |
|--|---------------|----------------|------------------------------------|-------------------------------------|----------------|
| HL ¹ | 0.02 | 1.25 | 16.0 | 784 | 1.046 |
| HL ¹ + Zn ²⁺ (1:1) | 0.18 | 7.29 | 24.7 | 112.5 | 1.094 |

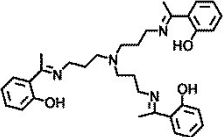
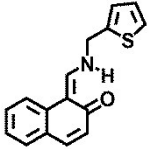
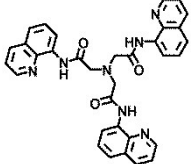
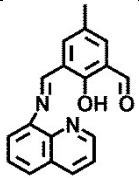
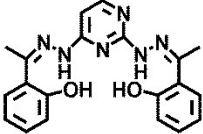
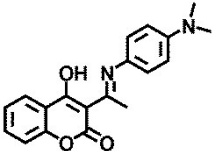
Values of k_r and k_{nr} for HL¹ and its 1:1 complex with Zn²⁺ are given in Table 1. We can see from the table that there are two opposing factors that determine the change in emission intensity of HL¹ and the metal complex; (i) large jump in k_r value on complex formation and (ii) higher non-radiative decay constant in the complex. The complexation of HL¹ with Zn²⁺ may give rigidity to the system and that leads to the increased k_r value and hence increase in emission intensity.

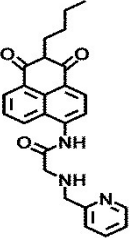
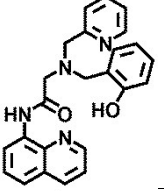
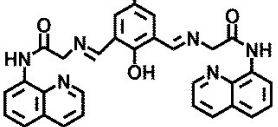
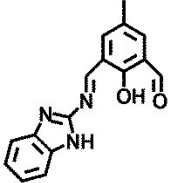
Lowest concentration of Zn²⁺ that can be measured in solution has been determined for both the Schiff-base ligands (Supporting Information, Fig. s16-s19). The limit of detection (LOD) of HL¹ and HL² for Zn²⁺ was determined by following 3σ method.⁴⁵ It has been found that LOD values of HL¹ and HL² are 0.832 and 0.474 nM, respectively. We have made comparison of recently published Zn²⁺ sensors with different aspects (Table 2). Our probe has several plus points and few limitations with respect to the others. Prime feature of our probe highlights its high sensitivity for Zn²⁺ ion. LOD values of HL¹ and HL² indicate that these molecules have lower values compared to others. While majority of the probes including present work have been synthesized by one step. Few of them cannot be used for cell-imaging study. However, comparing the excitation wavelengths, it can be noticed that HL¹ has higher excitation wavelength in the visible region. This is preferable for cell imaging study as excitation in UV region may induce cell-death.

Reversibility of Zn^{2+} has been checked (Fig. s20). Emission intensity of HL^1 has been measured in the presence of one eqv. of Zn^{2+} . Intensity increases as usual. In the presence of one eqv. of EDTA (disodium salt) reduces the intensity almost to the initial intensity of HL^1 . Again in the presence of Zn^{2+} , intensity of the probe increases. EDTA again decreases intensity and cycle goes on.

Fluorescence image and image under visible light of HL^1 in the presence various metal ions are given in Fig. s21. Under visible light, there is no distinct change in color of solution of HL^1 and HL^1 with different metal ions. However, few metal ions *e.g.* Zn^{2+} , Cd^{2+} , Mn^{2+} , Co^{2+} , Ni^{2+} and Cu^{2+} can generate pale yellow color with the Schiff-base compound.

Table 2: Comparison on few aspects of some recently published Zn-sensors

| Sl. No | Probe | No. of step for synthesis | Excitation (nm)/ Emission (nm) | LOD | Cell imaging study | Ref. |
|--------|---|---------------------------|--------------------------------|--------------|--------------------|------|
| 1 |  | 1 | 350/470 | 88 nM | No | 46 |
| 2 |  | 1 | 375/448 | 30 nM | Yes | 47 |
| 3 |  | 4 | 365/506 | 3.2 μ M | Yes | 48 |
| 4 |  | 1 | 430/539 | 5.81 nM | Yes | 29 |
| 5 |  | 1 | 375/469 | 0.69 μ M | No | 49 |
| 6 |  | 1 | 370/460 | 65.4 μ M | No | 50 |

| | | | | | | |
|----|---|---|---------|----------|-----|--------------|
| 7 |  | 2 | 360/522 | 7.2 nM | Yes | 51 |
| 8 |  | 3 | 370/510 | 66 nM | No | 52 |
| 9 |  | 1 | 360/482 | 0.1 μM | No | 53 |
| 10 |  | 1 | 445/528 | 0.832 nM | Yes | Present work |

Fluorescence image of HL¹ in the presence of Zn²⁺, Na⁺, K⁺, Cd²⁺, Hg²⁺, Pb²⁺, V³⁺, Mn²⁺, Fe³⁺, Co²⁺, Ni²⁺ and Cu²⁺ ions clearly shows that bluish green color is created only when Zn²⁺ is present with HL¹. Neither HL¹ nor the other metal ions can produce any change in color in fluorescence image. Thus, Zn²⁺ can be detected under UV irradiation. A visual change in color of the Schiff-base compound in the presence of Zn²⁺ ion under UV radiation can be a useful way for the “naked-eye” detection of the metal ion in solution.

Effect of pH on the emission intensity of HL¹ with and without one equiv. of Zn²⁺ has been checked in the range of 3.0 to 11.0 (Fig. 8). It is clear from the figure that there is almost no change in emission intensity of HL¹ in absence of Zn²⁺ in the pH range of 3.0-8.0. If we have close view on the emission intensity of HL¹ in absence of Zn²⁺ it can be seen very small increment in emission intensity has been occurred in pH higher than 8.0. However, pH has a significant effect on emission intensity of HL¹ in the presence of Zn²⁺. Emission intensity of HL¹ in the presence of Zn²⁺ has started to increase when pH of the medium is 4 or higher and reaches maxima at pH 8.0.

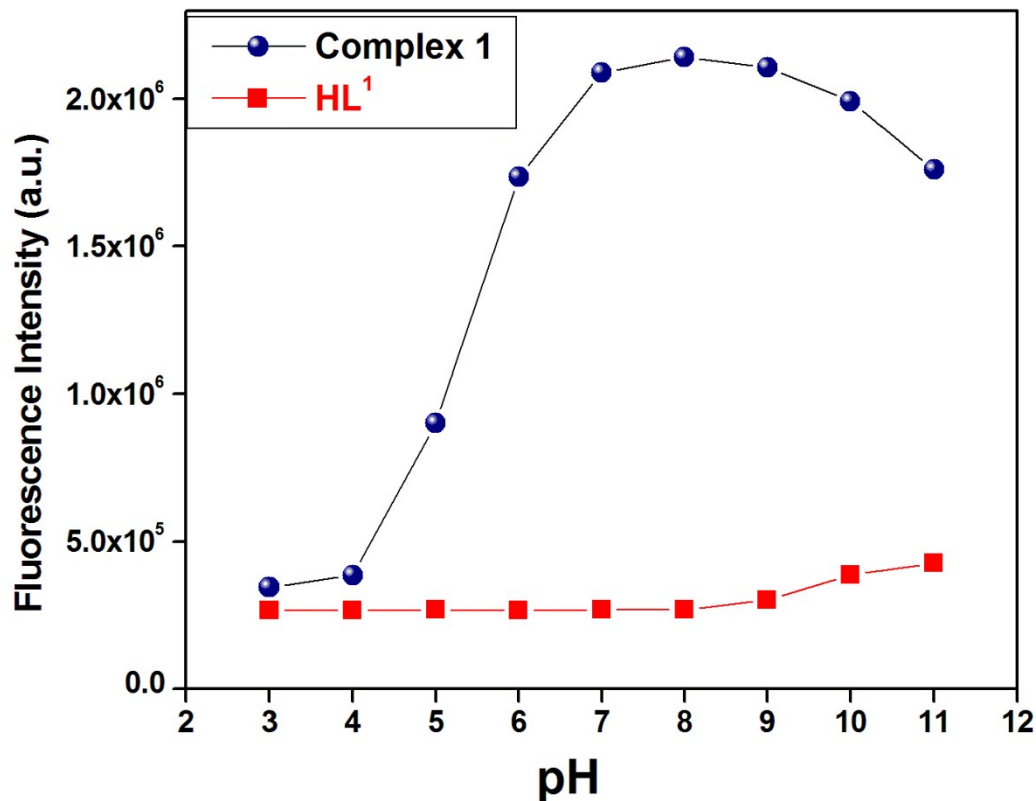


Fig. 8: Fluorescence intensity of HL¹ and HL¹ in the presence of Zn²⁺ at various pH. Red line with solid square box represents fluorescence intensity of HL¹ and blue line with solid round symbol represents fluorescence intensity of HL¹ in the presence of Zn²⁺.

NMR spectral studies

¹H NMR spectra of HL¹ were recorded in absence and in the presence of one equiv. of Zn²⁺ ion in DMSO-d₆ (Fig. 9). ¹H NMR spectrum of HL¹ shows very clear peaks. Peak for phenolic OH appears at $\delta = 12.87$ ppm. The diformyl compound undergoes Schiff-base condensation with one equivalent of 2-aminobenzimidazole leaving one CHO group unreacted. This is evident from the NMR spectrum of resulting compound which clearly displays a singlet peak at $\delta = 10.40$ ppm for one aldehyde proton. Imine proton appears at 9.65 ppm. Singlet peak corresponding to three protons at 2.33 ppm may be attributed to methyl group. Aromatic protons on phenyl and benzimidazolyl rings appear in the range of 7.99-7.19 ppm. Two singlet peaks at 7.99 and 7.73 ppm are due to the presence of two protons on benzene ring. However, no signal for NH proton was observed.

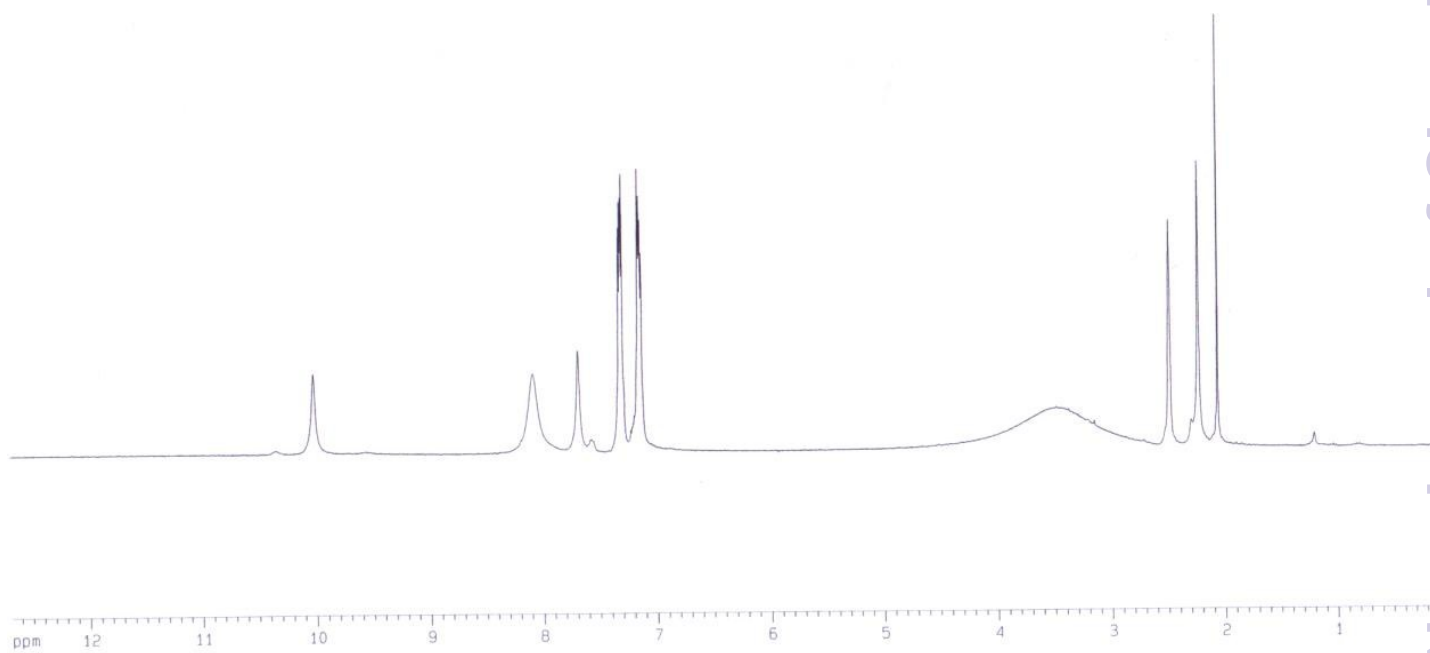
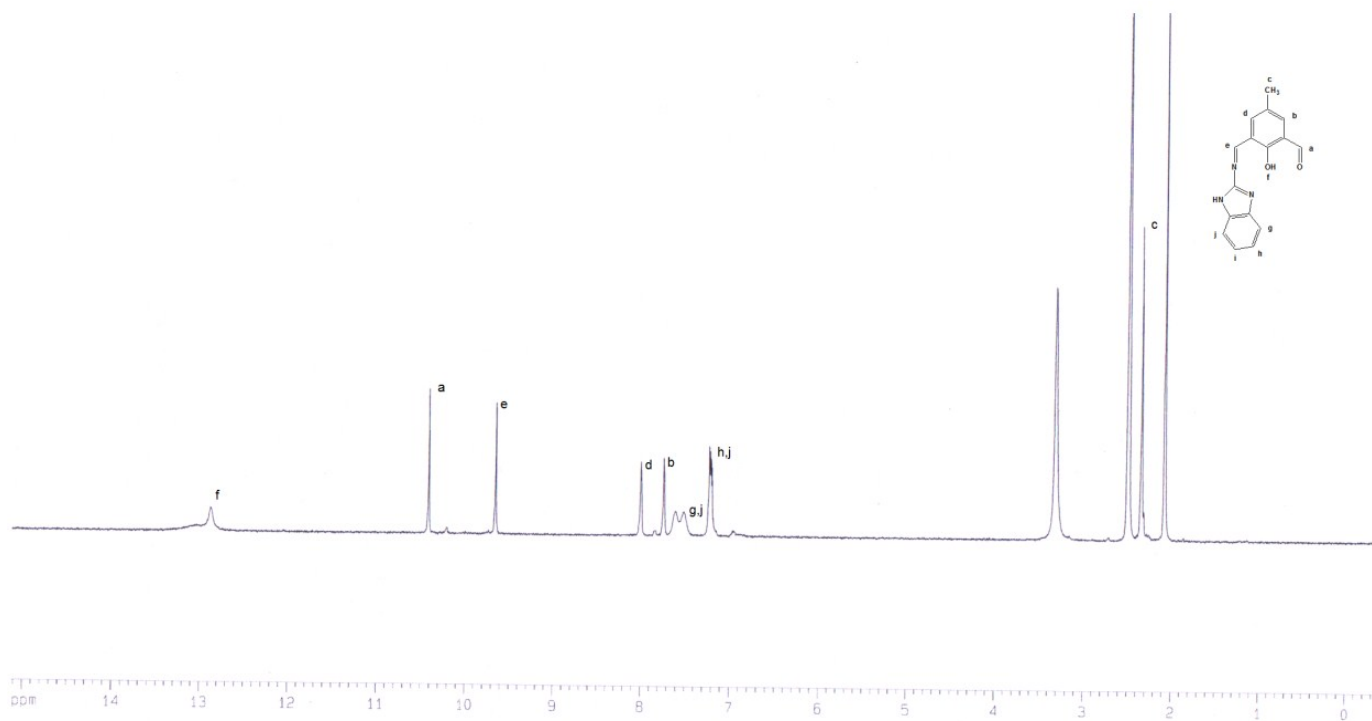


Fig. 9: ^1H NMR spectrum of HL¹ in absence (above) and in the presence of Zn²⁺ ion (below).

^1H NMR spectrum of HL^1 in the presence of Zn^{2+} ion is shown in Fig. 9. It exhibits many changes in the spectrum of HL^1 occurred due to the presence of Zn^{2+} . Peak for phenolic proton disappears here. Peak positions for CHO, imine and aromatic protons alter appreciably. Peak for one aldehyde proton has been obtained at 10.02 ppm. Methyl proton appears at 2.29 ppm. The changes in peak position may be attributed to the coordination of Zn^{2+} with HL^1 . Analysis of ^1H NMR spectra of HL^1 in the absence and in the presence of Zn^{2+} ion supports the proposed mechanism as depicted in Fig. 6. Change in position of imine proton and disappearance of phenolic proton indicate the coordination of the metal center with the imine nitrogen and phenoxo oxygen atoms. Thus, emission intensity enhancement due to PET mechanism is supported indirectly by the NMR spectra study.

Cell imaging study

The intracellular Zn^{2+} imaging behavior of HL^1 has been studied on A549, human lung cancer cell lines by fluorescence microscopy. After incubation with the probe (10 μM) at 37°C for 30 min, the cells display no intracellular fluorescence (Fig. 10B). However, cells exhibit light fluorescence with the addition of low concentration of zinc ion (10 μM) (Fig. 10C) and exhibited gradually intensive fluorescence when exogenous Zn^{2+} has been introduced into the cell *via* incubation with a zinc nitrate salt solution (50 μM) (Fig. 10D). The intensive fluorescence behavior has been, however, strongly suppressed when TPEN (100 μM) has been added to the medium. Since TPEN confers having a strong scavenging action on Zn^{2+} ion, the sensor molecules competitively inhibit to bind with Zn^{2+} ions, as a result, the intensive fluorescence disappears (Fig. 10F). This presents the confirmatory evidence of the sensor having the selectivity to sense Zn^{2+} ions. The fluorescence responses of the HL^1 with various concentrations of added Zn^{2+} proves that such fluorescence intensity can be used as indelible signature of selective sensor response clearly evident from the cellular imaging. Hence, these results indicate that HL^1 is an efficient candidate for monitoring changes in the intracellular Zn^{2+} concentration under biological conditions.

The cytotoxicity study (MTT assay) in human lung cancer cells treated with various concentrations of HL^1 for up to 6 h (Fig. s22) shows that HL^1 of concentration up to 10 μM does not show significant cytotoxic effects on human lung cancer cells for at least up to 6 h of its treatment. Further fixed concentration (10 μM) of HL^1 along with different concentrations of

zinc ions (10 μM and 50 μM) even do not show any significant cytotoxic effects on human lung cancer cells for up to 6 h as shown in Fig. s23. The study suggests that HL¹ can be readily used as an efficient, selective and sensitive tool for bioimaging at the indicated doses and incubation time without cytotoxic effects.

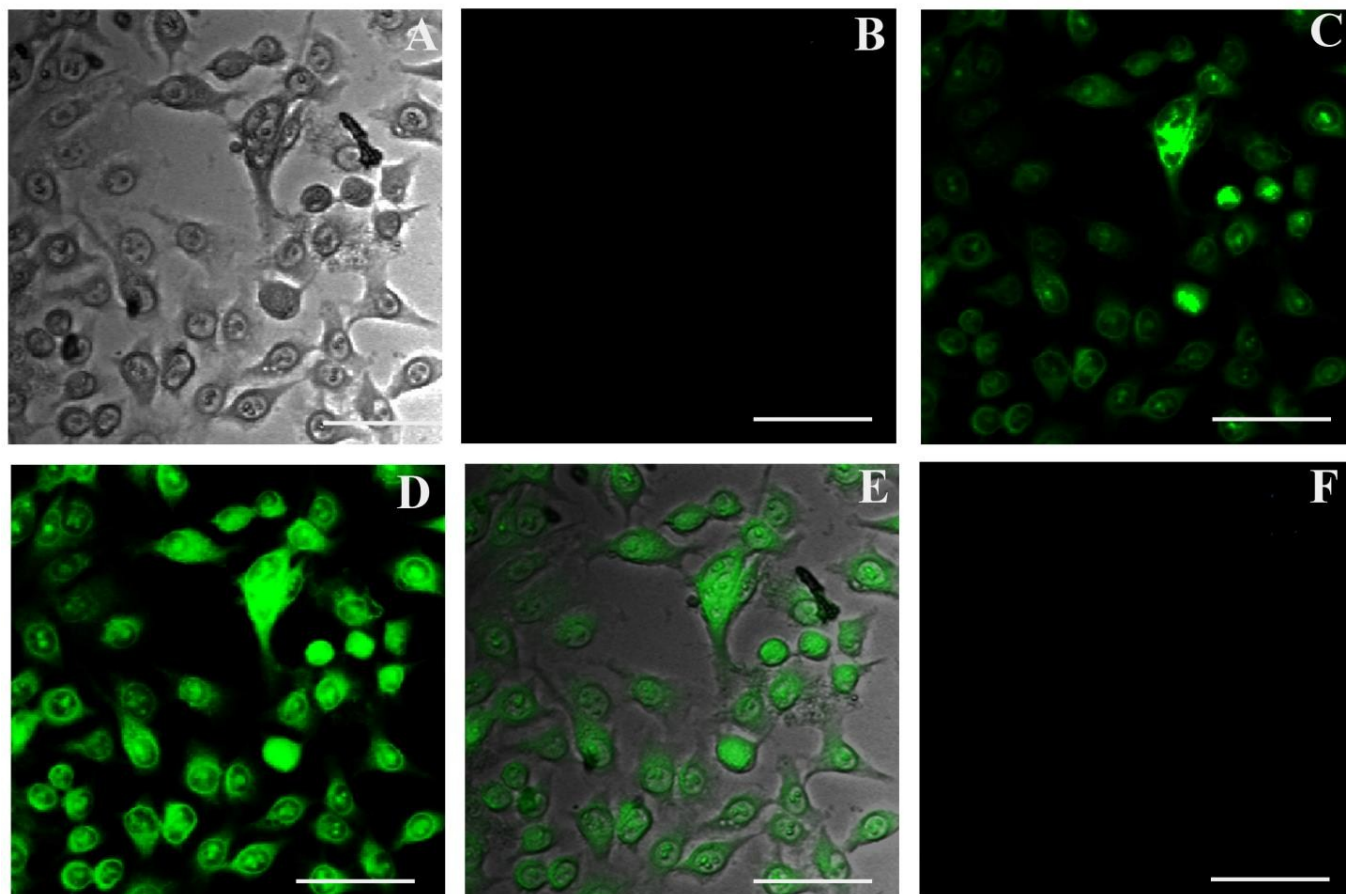


Fig. 10: (A) Phase contrast image, (B) fluorescence image of A549 cells incubated with 10 μM HL¹ for 30 min at 37°C. HL¹ (10 μM) incubated cells were washed with PBS and were exposed to the presence of sequentially increased concentrations of added extracellular Zn²⁺ ion as (C) 10 μM and (D) 50 μM . (E) Represent the merge image of phase contrast and fluorescence image. (F) Represent disappearance of fluorescence intensity in the A549 cells treated with the HL¹ and Zn²⁺ ion after further addition of 100 μM TPEN. For all imaging, the samples were excited at 445 nm (Scale bar represent 50 μm).

Conclusions

In summary, we have been able to establish 2-formyl-4-methyl-6-(2-benzimidazolyiminomethyl)phenol (HL¹) as a selective fluorescence sensor for Zn²⁺. Presence

of a methylene group in HL¹ has visible effect on UV-visible and fluorescence spectra in absence and in the presence of Zn²⁺. Emission intensity of HL¹ at 528 nm increases significantly in the presence of one eqv. of Zn²⁺. All other metal ions either reduce the emission intensity or induce no significant change in the intensity. However, with the presence of methylene group, we can tune spectral properties of such Schiff-base molecule. HL² with methylene group shows emission intensity at 478 nm with large change in peak position compared to HL¹. Both the Schiff-base molecules are highly sensitive for Zn²⁺ ion with very low LOD values. The compound has been used to study of cell imaging of cancer cell with cytotoxicity. Thus, easy to synthesis Schiff-base compounds can be used as selective chemosensor for Zn²⁺ and most importantly, the spectral properties of such compounds can be tuned accordingly.

Acknowledgements

PR wishes to thank Department of Science and Technology, New Delhi for financial support. SD thanks UGC, New Delhi for his fellowships. GPM is grateful to DST-PURSE Programme at University of Kalyani for financial support to complete a part of this work. Authors are thankful to Professor M. Ali, Department of Chemistry, Jadavpur University for providing facilities to record fluorescence spectra.

References:

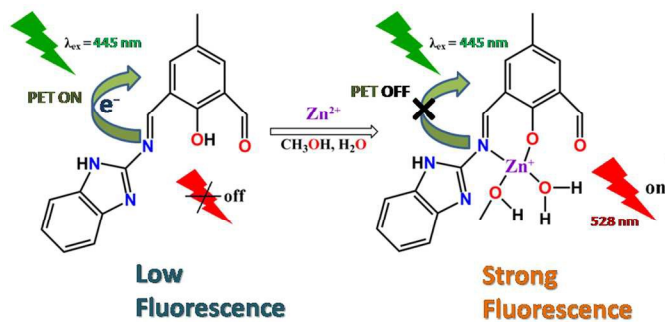
- 1 S. J. Lippard and J. M. Berg, *Principles of Bioinorganic Chemistry*, University Science Books, Mill Valley, CA 1994, p. 10, 14, 78.
- 2 J. E. Coleman, *Curr. Opin. Chem. Biol.*, 1998, **2**, 222.
- 3 S.C. Burdette and S.J. Lippard, *Proc. Natl. Acad. Sci. USA*, 100 2003, **100**, 3605
- 4 E. Kimura, S. Aoki, E. Kikuta and T. Koike, *Proc. Natl. Acad. Sci. USA*, 2003, **100**, 3731.
- 5 C. J. Frederickson, M. D. Hernandez and J. F. McGinty, *Brain Res.*, 1989, **480**, 317.
- 6 J.-Y. Koh, S. W. Suh, B. J. Gwag, Y. Y. He, C.Y. Hsu and D. W. Choi, *Science* 1996, **272**, 1013
- 7 A. I. Bush, W. H. Pettingell, G. Multhaup, M. D. Paradis, J. P. Vonsattel, J. F. Gusella, K. Beyreuther, C. L. Masters and R. E. Tanzi, *Science*, 1994, **265**, 1464.
- 8 M. Fried and D. M. Crothers, *Nucleic Acids Res.*, 1981, **9**, 6505.

- 9 A. Voegelin, S. Pfister, A.C. Scheinost, M.A. Marcus and R. Kretzschmar, *Environ. Sci. Technol.*, 2005, **39**, 6616.
- 10 J. Mertens, F. Degryse, D. Springael and E. Smolders, *Environ. Sci. Technol.*, 2007, **41**, 2992.
- 11 E. Callender and K.C. Rice, *Environ. Sci. Technol.*, 2000, **34**, 232.
- 12 Z. Xu, J. Yoon and D. R. Spring, *Chem. Soc. Rev.*, 2010, **39**, 1996.
- 13 C. J. Frederickson, E. J. Kasarskis, D. Ringo and R. E. Frederickson, *J. Neurosci. Methods*, 1987, **20**, 91.
- 14 W. Chyan, D. Y. Zhang, S. J. Lippard and R. J. Radford, *Proc. Natl. Acad. Sci., USA*, 2014, **111**, 143.
- 15 A. Loas, R. J. Radford S. J. Lippard, *Inorg. Chem.*, 2014, **53**, 6491.
- 16 D. Wang, X. Xiang, X. Yang, X. Wang, Y. Guo, W. Liu and W. Qin, *Sens. Actuators B*, 2014, **201**, 246.
- 17 E. M. Nolan, J. W. Ryu, J. Jaworski, R. P. Feazell, M. Sheng and S. J. Lippard, *J. Am. Chem. Soc.*, 2006, **128**, 15517.
- 18 K. Kikuchi, K. Komatsu and T. Nagano, *Curr. Opin. Chem. Biol.*, 2004, **8**, 182.
- 19 Y. Chen, Y. Bai, Z. Han, W. He and Z. Guo, *Chem. Soc. Rev.*, 2015, **44**, 4517.
- 20 D. Sarkar, A. K. Pramanik T. K. Mondal, *RSC Adv.*, 2015, **5**, 7647.
- 21 D. Y. Zhang, M. Azrad, W. Demark-Wahnefried, C. J. Frederickson, S. J. Lippard and R. J. Radford, *ACS Chem. Biol.*, 2015, **10**, 385.
- 22 G. R. C. Hamilton, L. Fullerton, B. McCaughan, R. F. Donnelly and J. F. Callan, *New J. Chem.*, 2014, **38**, 2823.
- 23 J. Ma, R. Sheng, J. Wu, W. Liu and H. Zhang, *Sens. Actuators B*, 2014, **197**, 364.
- 24 K. Komatsu, K. Kikuchi, H. Kojima, Y. Urano and T. Nagano, *J. Am. Chem. Soc.*, 2005, **127**, 10197.
- 25 K. Hanaoka, K. Kikuchi, H. Kojima, Y. Urano and T. Nagano, *Angew. Chem., Int. Ed.*, 2003, **42**, 2996.
- 26 P. Roy, K. Dhara, M. Manassero, J. Ratha and P. Banerjee, *Inorg. Chem.*, 2007, **46**, 6405.
- 27 B. Chakraborty, P. Halder, S. Chakraborty, O. Das and S. Paria, *Inorg. Chim. Acta*, 2012, **387**, 372.
- 28 T. Mistri, M. Dolai, D. Chakraborty, A. R. Khuda-Bukhsh, K. Kumar Das and M. Ali,

- Org. Biomol. Chem.*, 2012, **10**, 2380.
- 29 R. Alam, T. Mistri, A. Katarkar, K. Chaudhuri, S. K. Mandal, A. R. Khuda-Bukhsh, K. K. Das and M. Ali, *Analyst*, 2014, **139**, 4022.
- 30 S. Mandal, Y. Sikdar, D. K. Maiti, G. P. Maiti, S. K. Mandal, J. K. Biswas and S. Goswami, *RSC Adv.*, 2015, **5**, 72659.
- 31 C. Chen, G. Men, W. Bu, C. Liang, H. Sun, S. Jiang, *Sens. Actuators B*, 2015, **220**, 463.
- 32 L. Subha, C. Balakrishnan, S. Natarajan, M. Theetharappan, B. Subramanian and M.A. Neelakantan, *Spectrochim. Acta Part A*, 2016, **153**, 249.
- 33 R. R. Gagne, C. L. Spiro, T. J. Smith, C. A. Hamann, W. R. Thies and A. K. Schiemke, *J. Am. Chem. Soc.*, 1981, **103**, 4073.
- 34 D. D. Perrin, W. L. F. Armarego and D. R. Perrin, *Purification of Laboratory Chemicals*, Pergamon Press, Oxford, U.K., 1980.
- 35 A.M. Brouwer, *Pure Appl. Chem.*, 2011, **83**, 2213.
- 36 M. J. Frisch, G. W. Trucks, H. B. Schlegel, G. E. Scuseria, M. A. Robb, J. R. Cheeseman, J. A. Montgomery Jr., T. Vreven, K. N. Kudin, J. C. Burant, J. M. Millam, S. S. Iyengar, J. Tomasi, V. Barone, B. Mennucci, M. Cossi, G. Scalmani, N. Rega, G. A. Petersson, H. Nakatsuji, M. Hada, M. Ehara, K. Toyota, R. Fukuda, J. Hasegawa, M. Ishida, T. Nakajima, Y. Honda, O. Kitao, H. Nakai, M. Klene, X. Li, J. E. Knox, H. P. Hratchian, J. B. Cross, V. Bakken, C. Adamo, J. Jaramillo, R. Gomperts, R. E. Stratmann, O. Yazyev, A. J. Austin, R. Cammi, C. Pomelli, J. W. Ochterski, P. Y. Ayala, K. Morokuma, G. A. Voth, P. Salvador, J. J. Dannenberg, V. G. Zakrzewski, S. Dapprich, A. D. Daniels, M. C. Strain, O. Farkas, D. K. Malick, A. D. Rabuck, K. Raghavachari, J. B. Foresman, J. V. Ortiz, Q. Cui, A. G. Baboul, S. Clifford, J. Cioslowski, B. B. Stefanov, G. Liu, A. Liashenko, P. Piskorz, I. Komaromi, R. L. Martin, D. J. Fox, T. Keith, M. A. Al-Laham, C. Y. Peng, A. Nanayakkara, M. Challacombe, P. M. W. Gill, B. Johnson, W. Chen, M. W. Wong, C. Gonzalez and J. A. Pople, GAUSSIAN 03 (Revision C.02), Gaussian Inc., Wallingford, CT, 2004.
- 37 A.D. Becke, *J. Chem. Phys.*, 1993, **98**, 5648.
- 38 P.J. Hay and W.R. Wadt, *J. Chem. Phys.*, 1985, **82**, 299.
- 39 S. Miertus, E. Scrocco and J. Tomasi, *Chem. Phys.*, 1981, **55**, 117.
- 40 V. Barone, M. Cossi and J. Tomasi, *J. Comput. Chem.*, 1998, **19**, 404.

- 41 T. Mossman, *J. Immunol. Methods*, 1983, **65**, 55.
- 42 U. C. Saha, B. Chattopadhyay, K. Dhara, S. K. Mandal, S. Sarkar, A. R. Khuda-Bukhsh, M. Mukherjee, M. Helliwell and P. Chattopadhyay, *Inorg. Chem.*, 2011, **50**, 1213.
- 43 H.A. Benesi and J.H. Hildebrand, *J. Am. Chem. Soc.*, 1949, **71**, 2703.
- 44 A. Mallick and N. Chattopadhyay, *Photochem. Photobiol.*, 2005, **81**, 419.
- 45 V. Thomsen, D. Schatzlein and D. Mercurio, *Spectroscopy*, 2003, **18**, 112.
- 46 M. Hosseinia, A. Ghafarloob, M. R. Ganjali, F. Faridbod, P. Norouzi, M. S. Niasari, *Sens. Actuators B*, 2014, **198**, 411.
- 47 D. Karak, S. Das, S. Lohar, A. Banerjee, A. Sahana, I. Hauli, S. K. Mukhopadhyay, D. A. Safin, M. G. Babashkin, M. Bolte, Y. Garcia and D. Das, *Dalton Trans.*, 2013, **42**, 6708.
- 48 S. Goswami, A. K. Das, K. Aich, A. Manna, S. Maity, K. Khanra and N. Bhattacharyya, *Analyst*, 2013, **138**, 4593.
- 49 S. S. Mati, S. Chall, S. Konar, S. Rakshit, S. C. Bhattacharya, *Sens. Actuators B*, 2014, **201**, 204–212
- 50 D. Sarkar, A. K. Pramanik and T. K. Mondal, *RSC Adv.*, 2014, **4**, 25341.
- 51 T. Wei, J. Wang, Y. Chen and Y. Han, *RSC Adv.*, 2015, **5**, 57141.
- 52 E. J. Song, J. Kang, G. R. You, G. J. Park, Y. Kim, S.-J. Kim, C. Kim and R. G. Harrison, *Dalton Trans.*, 2013, **42**, 15514
- 53 Z. Dong, X. Le, P. Zhou, C. Dong and J. Ma, *RSC Adv.*, 2014, **4**, 18270.

Table of Content



A selective fluorescence chemosensor for Zn^{2+} has been developed with very low limit of detection value (0.832 nM).